

Bacterial population-level trade-offs between drought tolerance and resource acquisition traits impact decomposition

Ashish A. Malik^{1,2,3,*}, Jennifer B.H. Martiny³, Antonio Ribeiro⁴, Paul O. Sheridan^{2,5}, Claudia Weihe³, Eoin L. Brodie^{6,7}, Steven D. Allison^{3,8}

¹School of GeoSciences, University of Edinburgh, Edinburgh EH9 3FF, United Kingdom

²School of Biological Sciences, University of Aberdeen, Aberdeen AB24 3UU, United Kingdom

³Department of Ecology and Evolutionary Biology, University of California, Irvine, CA 92697, United States

⁴Centre for Genome-Enabled Biology and Medicine, University of Aberdeen, Aberdeen AB24 3UU, United Kingdom

⁵School of Biological and Chemical Sciences, University of Galway, Galway H91 TK33, Ireland

⁶Earth and Environmental Sciences, Lawrence Berkeley National Laboratory, Berkeley, CA 94720, United States

⁷Department of Environmental Science, Policy and Management, University of California, Berkeley, CA 94720, United States

⁸Department of Earth System Science, University of California, Irvine, CA 92697, United States

*Corresponding author: Ashish A. Malik, School of GeoSciences, University of Edinburgh, Office 204, Crew Building, The King's Buildings, Alexander Crum Brown Road, Edinburgh EH9 3FF, United Kingdom. Email: ashish.malik@ed.ac.uk

Abstract

Microbes drive fundamental ecosystem processes, such as decomposition. Environmental stressors are known to affect microbes, their fitness, and the ecosystem functions that they perform; yet, understanding the causal mechanisms behind this influence has been difficult. We used leaf litter on soil surface as a model *in situ* system to assess changes in bacterial genomic traits and decomposition rates for 18 months with drought as a stressor. We hypothesized that genome-scale trade-offs due to investment in stress tolerance traits under drought reduce the capacity for bacterial populations to carry out decomposition, and that these population-level trade-offs scale up to impact emergent community traits, thereby reducing decomposition rates. We observed drought tolerance mechanisms that were heightened in bacterial populations under drought, identified as higher gene copy numbers in metagenome-assembled genomes. A subset of populations under drought had reduced carbohydrate-active enzyme genes that suggested—as a trade-off—a decline in decomposition capabilities. These trade-offs were driven by community succession and taxonomic shifts as distinct patterns appeared in populations. We show that trait-trade-offs in bacterial populations under drought could scale up to reduce overall decomposition capabilities and litter decay rates. Using a trait-based approach to assess the population ecology of soil bacteria, we demonstrate genome-level trade-offs in response to drought with consequences for decomposition rates.

Keywords: bacteria, drought, genomics, litter decomposition, microbial traits, population ecology

Introduction

Microbes drive large-scale processes, such as the global biogeochemical cycling of elements. Environmental stress can influence cellular-level functions in microorganisms with consequences for these processes. However, determining the quantitative impacts of environmental stressors on the physiological response of microbes is extremely challenging. A trait-based approach, akin to that widely used in plant ecology [1, 2], offers the opportunity to functionally characterize and represent the enormous diversity of microbes involved in system-level processes.

Traits are an organism's phenotypic characteristics that govern process rates [3, 4]. By focusing on the phenotypic aspects of microbes rather than their taxonomic identity, trait-based approaches provide a way forward to integrate functional information across species, space, and time. Quantitative phenotypic measurements have been made successfully at the community

level, for example of carbon use efficiency [5], but may not be feasible for single microbial populations in environments, such as soil. However, we can use genetic markers to study traits in populations of single species or strains by leveraging new genome assembly and binning approaches that make it possible to extract hundreds of microbial genomes (metagenome-assembled genomes or MAGs) from environmental microbiomes [6, 7].

Modern omics technologies have transformed microbial ecology by providing a granularity needed to study complex and highly diverse environmental microbiomes [8, 9]. However, linking microbiome characteristics to ecosystem processes or to changes in pools and fluxes has remained difficult [10]. This scaling limitation may be in part because of methodological challenges in testing how environmental factors affect individual- or population-level physiology, which ultimately impacts microbial fitness and contribution to ecosystem functioning. For instance,

Received: 16 July 2024. Revised: 15 October 2024. Accepted: 1 November 2024

© The Author(s) 2024. Published by Oxford University Press on behalf of the International Society for Microbial Ecology.

This is an Open Access article distributed under the terms of the Creative Commons Attribution License (<https://creativecommons.org/licenses/by/4.0/>), which permits unrestricted reuse, distribution, and reproduction in any medium, provided the original work is properly cited.

shotgun sequencing approaches often produce community-aggregated traits that represent the additive properties of phylogenetically diverse members of the community, which may not reflect emergent properties resulting from complex interactions among community members and their environment [4, 11]. Thus, the measured microbial and environmental characteristics may be decoupled. Therefore, there is a need to study microbial traits at multiple levels of biological organization—from populations of a species/strain to collective communities—to better understand and predict the ecosystem-level impacts of microbial processes.

Traits can trade-off due to adaptive physiological processes in response to short-term fluctuations in the environment. Physiological constraints in stressful conditions, such as reduced water availability, could lead to greater cellular-level allocation of resources to maintenance and survival, relative to resource acquisition traits [12]. If the environmental stressors persist over longer time periods, these will manifest as genome-encoded trade-offs across populations through ecological selection or evolutionary processes [13, 14]. Reduced resource acquisition traits at the community level can have system-level impacts, such as reduction in decomposition rates. However, such ecosystem-level quantifications or predictions are hard to make due to mismatches in functional response at different levels of biological organization. Various ecological and abiotic factors may impact the emergent community response, potentially reinforcing or attenuating the population-level trade-offs in traits.

Climatic extremes, such as drought, are becoming more frequent and severe, and act as stressors for microbial decomposers. Drier environments are thought to reduce microbial activity and therefore organic matter decomposition [15, 16]. Drought-induced reduction in microbial activity may occur due to organismal responses to water stress as well as due to limitations on resource diffusion and transport [15, 16]. Drought is known to change the composition of active members of the microbial community through environmental filtering, as selective pressures enable some taxa to gain competitive advantage over others [17–19]. Microorganisms also have the potential to acquire new genes through horizontal gene transfer or homologous recombination [20]. Such evolutionary processes could enable organisms under chronic drought to gain stress tolerance traits. This functional diversification through generation of new genetic variation without shifting community taxonomic composition highlights why linking of microbial and ecosystem processes could be better achieved through trait-based approaches.

While population-level data can help predict the organismal response to stress, the emergent community-level response is the most relevant at the ecosystem scale. If population-level traits simply add up, the effect of stress on genomic traits in microbial populations and trade-offs with fitness traits should scale up to the community-level. We used long-term drought as a persistent stress on microbes that grow on plant leaf litter to investigate the impact of stress on microbial traits at the population level and its impact on emergent community traits that influence rates of litter decomposition. We hypothesized that drought imposes constraints on the metabolism of decomposer populations, such that increased investment in stress tolerance traits reduces resource acquisition traits. This trade-off scales up to reduce the emergent community-level decomposition capabilities and decrease rates of organic matter decomposition.

We measured traits in populations of single species or strains, and collective communities in an *in-situ* decomposition experiment in Mediterranean grassland and shrubland ecosystems. We used two different litter types to assess if microbial drought response strategies differ across litter types of divergent chemical

quality. The study was performed in litter bags of 1 mm mesh size that were placed on the soil surface in experimental plots with ongoing drought treatment. Genomic traits of the decomposer community in litter bags were measured using shotgun metagenomics at four time points over an 18-month period (Fig. S1). We used bacterial MAGs to represent populations of single species or strains and probed for trade-offs in traits using the frequencies of genes linked to traits of interest. The abundance of these populations in communities across treatments was used to compare trait trade-offs at the population and community levels. This rarely used approach tests if patterns across biological levels are scale-dependent and helps better understand the ecosystem-level implications for microbial decomposition.

Materials and methods

Field site

We performed a leaf litter decomposition experiment in the field at the Loma Ridge Global Change Experiment situated near Irvine, California, USA (33°44'N, 117°42'E, 365 m elevation). The site experiences a Mediterranean climate (mean annual temperature: 17°C, mean annual precipitation: 325 mm) with a summer drought from May to October and periods of precipitation from November to April. The vegetation at the site consists of an annual grassland adjacent to a coastal sage scrub ecosystem [21, 22]. The long-term experiment consisted of grassland plots (6.7 × 9.3 m) with native perennial grass *Stipa pulchra*; exotic annual grasses, such as *Avena*, *Bromus*, *Festuca*, and *Lolium*; and forbs, such as *Erodium* and *Lupinus*. The shrubland plots (18.3 × 12.2 m) host crown-sprouting shrub species, such as *Salvia mellifera*, *Artemisia californica*, *Eriogonum fasciculatum*, *Acmispon glaber*, and *Malosma laurina* [21, 23]. We used the long-term drought experimental plots that received continuous field precipitation manipulations since 2007; reduced precipitation treatment plots were covered with retractable clear polyethylene rain shelters during a subset of precipitation events during the wet season to achieve ~40% precipitation reduction compared to ambient plots (Fig. S1). We used a total of 16 plots consisting of four replicated plots per treatment of grassland ambient, grassland reduced, shrubland ambient and shrubland reduced.

Experimental design

Litter of four types was collected from each treatment on 30 August 2017. Litter from all replicated plots ($n=4$) within each treatment was homogenized by hand mixing. To make litter bags, dry, senescing sheath and blade material in grassland was cut to a length of ~10 cm, whereas freshly fallen intact dry leaves were used in shrubland. In total, 6 g dry litter mass was placed into 15 cm × 15 cm bags of 1 mm mesh window screen. Litter bags were deployed in the field on 12 September 2017; they were placed on top of the soil surface under the canopy. Sixteen litter bags were collected at each time point (Fig. S1): 30 November 2017 (T1; end of the dry season), 11 April 2018 (T2; end of the wet season), 16 July 2018 (T2.5; middle of the dry season; additional sampling point only to measure litter mass loss), 5 November 2018 (T3; end of the dry season) and 19 February 2019 (T4; end of the wet season). Litter in each bag was weighed at the start of the experiment and at each sampling point. A subsample was dried to constant mass at 65°C to obtain the moisture content and dry mass of litter. Mass loss is reported as percentage initial dry mass.

Deoxyribonucleic acid extraction and sequencing

Deoxyribonucleic acid (DNA) was extracted from a coarse-ground litter aliquot of 50 mg for time points T1, T2, T3 and T4 (total

samples: 64). We used ZymoBiomics DNA isolations kits (Zymo Research, Irvine, CA, USA) and followed manufacturer instructions. Sample was homogenized by bead beating for 5 min at maximum speed (6.0 m/s, FastPrep-24 High Speed Homogenizer, MP Biomedicals, Irvine, CA, USA). Purity and concentration of extracted DNA was assessed using gel electrophoresis, a Qubit fluorometer (LifeTechnologies, Carlsbad, CA, USA) and Nanodrop 2000 Spectrophotometer (Thermo Scientific, USA). Metagenomics library preparation and sequencing were carried out at the DNA Technologies and Expression Analysis Cores at the University of California Davis Genome Center. We used PE150 sequencing on NovaSeq System (Illumina, San Diego, CA, USA) with the default insert size of 250–400 bp.

Reads-based analysis to obtain community-level functional gene abundances

To get a reads-based assessment at the community-level, DNA sequences were annotated with the Metagenomics Rapid Annotation using Subsystems Technology (MG-RAST) server version 4.0.3 [24]. Functional annotations were performed with the SEED Subsystems database and taxonomic classification up to genus level was performed using the RefSeq database (maximum e-value cut-off of 10^{-5} , minimum identity cut-off of 60% and minimum length of sequence alignment of 15 nucleotides).

Metagenomic co-assembly, binning, and annotation of prokaryotic genomes

For population-level analysis of genetic traits, the goal was to retrieve a high number of MAGs by *de novo* assembly and binning. To achieve this, we used a co-assembly approach merging the four replicates per treatment. Metagenome Orchestra-MAGO (version V2.2b; 2020-03-08) [25] was used to produce MEGAHit (version 1.2.8) [26] co-assemblies. Quality control and trimming approaches were like those used for individual assemblies. To extract prokaryotic bins from co-assemblies, we used the binning module of MetaWRAP (version 1.2.1) [27], MetaBAT2 (version 2.12.1) [28], Concoct (version 1.0.0) [29], and Maxbin2 (version 2.2.6) [30]. MetaWRAP's downstream modules were run over the collected bins with thresholds of minimum 45% completion and maximum 10% contamination obtaining bin-related statistics using CheckM (version 1.0.12) [31]. For the resulting bins, carbohydrate active enzymes (CAZy) were annotated using dbCAN2 (version 2.0.11) [32] with default parameter values. To obtain KEGG orthology (KO) annotations for the bins, we used Prodigal (version 2.6.3) [33] to carry out gene-calling over the bins and output was then used to query the Kofam database (ftp://ftp.genome.jp/pub/db/kofam/) with kofamscan (version 1.2.0) [34] using default parameter values. The quant_bins module of MetaWRAP (version 1.2.1) was used to compute the abundances of bins across samples.

Statistical analysis and visualizations

Statistical significance of decomposition rates measured as litter mass loss was estimated across vegetation and precipitation treatments using multivariate analysis of variance (ANOVA). Multivariate ANOVA was also used to assess the effect of vegetation, precipitation and the interaction of the two factors across all time points on the different categories of functional genes (level 1 of SEED Subsystems classification). Categories of functional genes with the highest and most statistically significant fold changes in read abundance in reduced precipitation treatment compared to the ambient were identified as drought-enriched functions. Fold

change was estimated as the ratio of sum-normalized read abundance in reduced and ambient precipitation treatments averaged across all time points and vegetation types. Statistical significance of this change with precipitation was estimated using one-way ANOVA across the precipitation treatments. Three functional categories with $P < .001$ were identified: membrane transport, stress response, and iron acquisition and metabolism. We then used differential abundance analysis carried out using DESeq2 [35] with precipitation as the experimental condition to identify the individual drought-enriched functional genes within the three categories. The temporal pattern and treatment effect of the three drought-enriched functional groups was visualized using line plots. Statistical significance of change with precipitation treated at each time point was estimated using one-way ANOVA. Temporal pattern and treatment effect of individual drought-enriched functional genes were visualized using a heatmap created with the pheatmap package [36]; more descriptive level 2 functional annotation of each gene was highlighted using a color code.

To demonstrate gene level trade-offs between drought-enriched genes and genes for decomposition, we made scatter plots with the sum of normalized copy numbers for multiple genes representing the three abundant drought responsive gene functions on the x-axis and normalized total number of CAZy genes on the y-axis. Normalization was performed using the total gene number per genome, which accounted for genome size and bin completeness. Trade-offs were visualized as negative regressions, displayed on the scatter plot using regression lines. Bacterial MAG-level gene copy numbers for total CAZy genes and drought enriched genes across treatments were visualized using geom_point and geom_smooth lm function. Bacterial MAG count for variable gene copy numbers for total CAZy genes and drought enriched genes were plotted with geom_histogram; geom_vline function was used to indicate the mean gene copy number across all MAGs. Wilcoxon signed rank sum test was used to examine the statistical differences in gene copy number across the precipitation treatments. The trade-offs in resource acquisition and stress tolerance traits were plotted with geom_point and geom_smooth lm functions. Here, only a subset of the MAGs from each treatment were plotted; these were MAGs that were differentially abundant in drought samples compared to the ambient control and vice versa. Trade-offs visualized as negative regressions were displayed on the scatter plot using regression lines. Abundance of MAGs in metagenomes was obtained using the quant_bins function expressed as genome copies per million reads and visualized as the size of each point representing the mean abundance over the four time points. The temporal pattern of these differentially abundant MAGs across the different treatments was plotted as a heatmap with the pheatmap package; phylum-level affiliation of each MAG was highlighted using a color code. MAGs were labelled as per their family-level affiliation; when this was not available a coarser taxonomic classification at the level of order or phylum was used. All visualizations were made in ggplot2 package [37] in R 3.4.2 [38].

Results and discussion

Ecosystem-level decomposition rates under drought

Drought is known to negatively impact decomposition in Mediterranean semi-arid ecosystems, including in multiple prior studies at our experimental site [39–42]. However, in our experiment, litter decomposition rates were statistically unaffected by

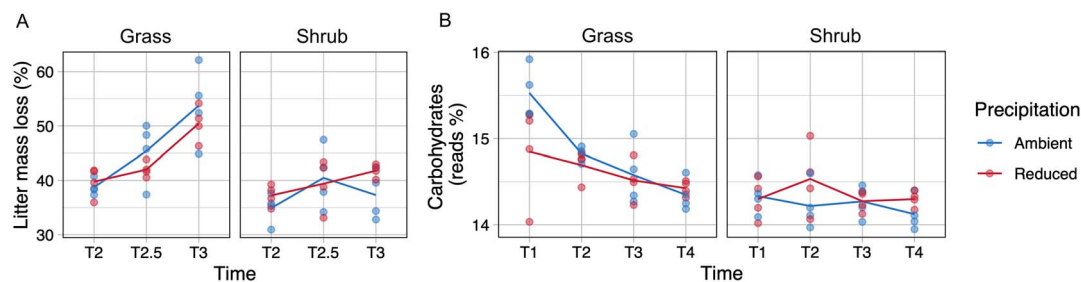


Figure 1. Effect of drought on decomposition rates and community decomposition capabilities. (A) Decomposition rates measured as percentage loss of litter mass since the start of the litter bag experiment. (B) Temporal patterns of community-aggregated read abundance of functional genes belonging to the carbohydrates category.

long-term drought (Fig. 1A; ANOVA $P > .05$), although there was a non-significant trend toward lower decomposition rates in grass litter under reduced precipitation treatment compared to the ambient control. After 14 months of *in situ* experimental incubation in the grassland system, mass loss under reduced precipitation treatment was $50.5 \pm 3.3\%$ compared to $53.8 \pm 7.2\%$ under ambient precipitation treatment. Decomposition rates were significantly lower in shrub litter (ANOVA $P < .001$) likely due to its higher C:N ratio, higher proportion of lignin and lower proportion of cellulose, hemicellulose and soluble compounds than the grass litter [43]. After 14 months, mass loss in the shrubland system under reduced precipitation treatment was $41.8 \pm 1.2\%$ compared to $37.3 \pm 4.5\%$ under ambient precipitation treatment. Litter mass loss measures showed abnormally high variability due to soil infiltration into the litter bags, which could have affected the accuracy of the rate estimates (especially at T4, 18 months of incubation; this time point was excluded). Litter decomposition rates from other experiments performed at the same site using litter bags with smaller mesh size have found lower decomposition rates in grass litter under drought [22, 44], and therefore we are confident that drought generally decreases decomposition at our site.

Metagenomic sequencing across the four sampled time points was used to investigate microbial community-level patterns in trait variation during decomposition. We assessed changes in community-level functional gene abundance using metagenomic reads annotated with SEED Subsystems databases. The category of level 1 functions called carbohydrates (consisting of genes for carbohydrate decomposition but also the central carbon metabolism and fermentation pathways) was not significantly different across the precipitation treatment, although there was a vegetation-precipitation interaction effect (ANOVA: vegetation $P < .001$, precipitation $P = .52$, vegetation \times precipitation $P = .02$), which could mean that it was negatively affected by the precipitation treatment only in the grass litter communities and not in the shrub litter communities (Fig. 1B). Carbohydrate gene abundance was significantly lower in shrub litter communities compared to grass litter communities (ANOVA: $P < .001$). This pattern of carbohydrate genes across the vegetation and precipitation treatments largely reflects the overall pattern of decomposition rates observed at our study site.

Community-level drought stress response linked to osmotic adaptations and iron metabolism

From the analysis of metagenomics-derived community-level functional gene abundance, three categories of level 1 functions in Subsystems classification were significantly higher in the drought treatment relative to ambient (Fig. 2A): membrane transport (ANOVA: vegetation $P < .001$, precipitation $P < .001$,

vegetation \times precipitation $P = .99$), stress response (ANOVA: vegetation $P < .001$, precipitation $P < .001$, vegetation \times precipitation $P = .7$), and iron acquisition and metabolism (ANOVA: vegetation $P < .001$, precipitation $P < .001$, vegetation \times precipitation $P = .44$). In microbial communities from both grass and shrub litter, sequence reads annotated to these three categories were consistently higher in drought treatment at most time points (Fig. 2B) suggesting a similar drought response in very distinct communities [23, 45]. Individual genes belonging to the three drought-enriched functional categories were linked to oxidative and osmotic stress, antiporters, ABC transporters, protein secretion systems and siderophores (Fig. S2). Enrichment of these genes is consistent with our hypothesis and other studies of bacterial drought response pathways [45–47].

Drought responsive traits of bacterial populations

To investigate drought responsive traits in bacterial populations, we analyzed gene profiles in MAGs retrieved by *de novo* assembly and binning. Overall, we retrieved 533 bacterial MAGs with contamination of $< 10\%$ and completeness of $> 45\%$ (207 MAGs had completeness of $> 70\%$). These MAGs spanned all major bacterial phyla. In some cases, multiple MAGs were retrieved for a species, which indicates strain-level genomic resolution; hence we consider MAGs representative of populations. For each MAG, we obtained gene copy numbers with KEGG annotations. From each of the three categories of functional genes that were most responsive to drought treatment at the community level (Fig. 2), we chose the most abundant genes and queried for them in MAGs to assess whether they were present in higher copy numbers in populations under drought (gene copy numbers were normalized to account for variable genome size and bin completeness). We used the sum of copy numbers for the following set of genes and refer to them as drought responsive functions: (i) Na⁺:H⁺ antiporter in the “membrane transport” category (Na⁺:H⁺ antiporter NhaA, NhaB, and NhaC family; multicomponent Na⁺:H⁺ antiporter subunit A, B, C, D, E, F and G), (ii) glycine transport in the “stress response” category (glycine betaine/proline transport system ATP-binding protein, permease protein and substrate-binding protein; choline/glycine/proline betaine transport protein; glycine betaine transporter; D-serine/D-alanine/glycine transporter) and (iii) Fe³⁺ transport in the “iron acquisition and metabolism” category (ferric enterobactin transport system substrate-binding protein, permease protein and ATP-binding protein; ferric hydroxamate transport system substrate-binding protein and permease protein; ferric transport system ATP-binding protein, permease protein and substrate-binding protein).

For all three drought responsive functions, mean gene copy numbers were higher in bacterial MAGs from drought

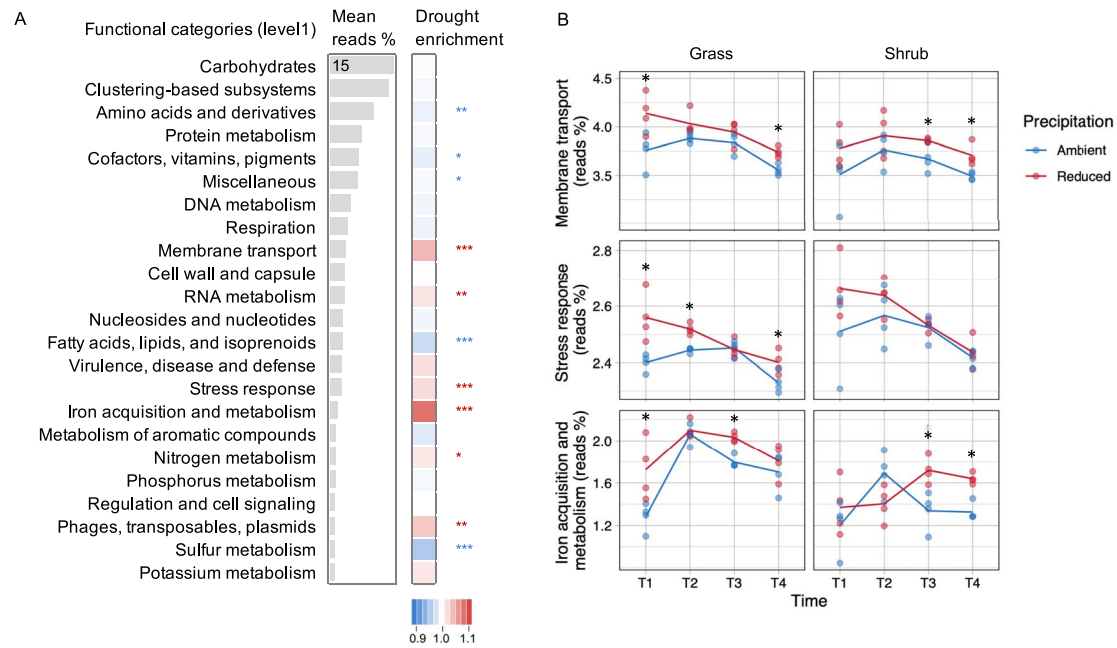


Figure 2. Community-level drought-enriched functional categories. (A) Results of community-aggregated read abundance-based analysis of major categories of functional genes in grass and shrub litter across all time points. This differential abundance analysis highlighted the drought-enriched functional categories that were significantly higher in the reduced precipitation treatment compared to ambient. The bar plot shows mean read abundance and heatmap shows the fold change in response to drought. Asterisks indicate significant drought enrichment measured as pairwise variation between ambient and reduced precipitation treatments (** $P < .001$, ** $P < .01$, * $P < .05$). (B) Temporal patterns of community-aggregated read abundance across treatments for the most drought-responsive categories of functional genes: membrane transport, stress response, and iron acquisition and metabolism. Asterisks indicate significant pairwise difference between ambient and reduced precipitation treatments at each time point (* $P < .05$).

communities relative to control in both grass and shrub litter (Fig. 3A–C). This difference suggests that bacterial populations under drought have increased gene copy numbers for key stress tolerance traits, which likely improved their fitness under drought, consistent with our hypothesis. Membrane transport functions performed by Na⁺:H⁺ antiporter subunit A in maintaining monovalent cation and proton homeostasis could be crucial for drought stress tolerance, a mechanism that has been identified in microbes and plants to tolerate drought and salinity stress [48–50]; we have previously reported this adaptation in our study at the same field site using metatranscriptomics [45]. Differential abundance of genes for transport of osmolytes, such as glycine betaine and proline, under osmotic stress has been well documented in laboratory cultures and to some extent in soils [51, 52]. These genes are related to maintenance of intracellular osmotic potential by increasing the concentrations of organic compatible solutes. In addition to triggering osmotic stress, drought appears to reduce iron availability in microorganisms due to reduced diffusion and increased aeration that oxidizes Fe²⁺ into insoluble Fe³⁺. We demonstrate higher abundance of genes for iron transport and metabolism (e.g. Fe³⁺ siderophore transport system) presumably as a metabolic adaptation to mitigate iron limitation caused by drought [53–55]. Here, we used community-level drought-responsive functions to inform MAG-level functional gene analysis. A more robust statistical analysis that focusses directly on MAGs may identify other drought responsive functions in bacterial populations.

Trade-offs between stress tolerance and resource acquisition traits across populations

We tested whether increased investment in stress tolerance traits in populations under drought (measured here in terms of higher gene copy numbers for drought responses) leads to

lower decomposition capabilities. To demonstrate such a tradeoff, we quantified the total number of CAZyme (carbohydrate-active enzyme) genes in the recovered MAGs; CAZyme genes are involved in decomposition of carbohydrates [56], a major substrate in grass and shrub litter. A trade-off between drought tolerance and resource acquisition traits would manifest as a negative correlation between counts of genes representing the two traits, with the slope determining the magnitude of this trade-off. We expected to see this trade-off for populations under both drought and control treatments due to long-term evolutionary changes [13, 14], but we anticipated that the magnitude of the trade-off would be higher under drought due to stronger short-term selection for drought tolerant populations.

We observed statistically significant negative relationships in grassland bacterial MAGs, and the slopes were either similar or more negative in the drought treatment compared to control (Fig. 3D–F). In other words, populations in grass litter with higher gene copy numbers for the drought responsive functions had lower total CAZyme genes, consistent with our trade-off hypothesis. This pattern was also seen in bacterial populations from shrub litter (Fig. 3D–F), but it was weaker compared to populations from grass litter. The negative relationship between Fe³⁺ transport genes and total CAZyme genes was strongest and statistically significant in drought treatments from both grass and shrub litter, likely because “iron transport and metabolism” was the most highly enriched functional gene category in response to drought in both grass and shrub communities (Fig. 2). We also observed that a higher number of bacterial MAGs in grass litter under drought compared to ambient had a lower count of CAZyme genes (Fig. 3G). Such a drought-linked pattern was not observed for bacterial MAGs from shrub litter (Fig. 3G). The negative relationship between drought-enriched genes and total CAZyme genes demonstrates the presence of a gene-level tradeoff between stress

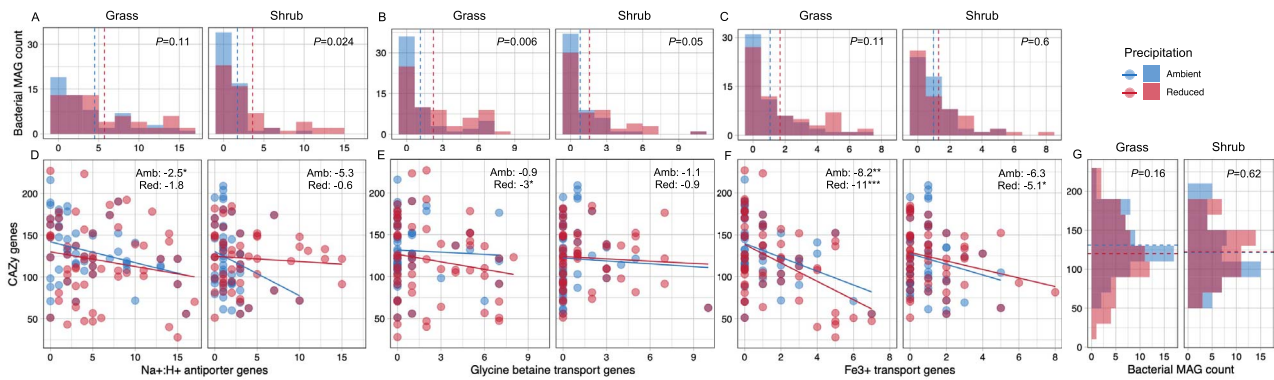


Figure 3. Gene copy numbers of drought responsive functions within MAGs and their trade-offs with CAZy genes. (A–C) Histograms showing the count of all bacterial MAGs with varying number of genes for the drought-enriched functions: Na⁺:H⁺ antiporter (A), glycine betaine (B), and iron transport (C). The vertical dotted lines represent mean number of genes in MAGs from ambient and reduced precipitation treatment. Also presented are the P values of Wilcoxon signed rank sum test to highlight statistical differences in number of genes across the precipitation treatments. (D–F) Scatter plot of number of genes for drought-enriched functions in each MAG on the x-axes and total CAZy genes on the y-axes with linear regression lines for ambient and reduced precipitation treatment. Also presented are the slope values for each regression and asterisks, which indicate significant negative correlation of drought enriched genes and CAZy genes (** $P < .001$, * $P < .01$, * $P < .05$). (G) Histogram showing the count of bacterial MAGs with varying number of CAZy genes. The horizontal dotted lines represent mean number of genes in MAGs from ambient and reduced precipitation treatment and statistical differences are highlighted using P values of the Wilcoxon signed rank sum test.

tolerance and resource acquisition traits in bacterial populations. Such trade-offs have been theorized [12] to act at the level of populations, and here we provide empirical evidence in support of that theory for bacteria.

Trade-offs across populations of drought-responsive bacteria

To assess the implications of gene-based trade-offs across populations, we examined the influence of reduced precipitation on the abundance of bacterial populations over the 18-month decomposition experiment. Abundance of populations (individual MAGs) was quantified as genome copies per million metagenomic reads across all samples. Instead of analyzing all populations that were present in the precipitation treatments as in Fig. 3, we identified drought-selected populations as MAGs that were significantly more abundant in drought samples compared to the ambient control and vice versa. We obtained the following number of MAGs that were differentially abundant in each treatment: grass ambient precipitation: 25, grass reduced precipitation: 23, shrub ambient precipitation: 9, shrub reduced precipitation: 18 (low abundance MAGs with <5 genome copies per million reads were excluded). For each MAG, we used the sum of copy numbers for the genes representing all three drought responsive functions as a measure of drought stress tolerance and plotted it against total CAZyme genes (Fig. 4A) while also accounting for the taxonomic affiliation of each MAG at the level of family (coarser level when this was not available). We demonstrate that population level trade-offs were only observed in grass litter under drought and that these trade-offs were driven by taxonomic shifts across treatments.

Drought-selected populations in grass litter belonging to the taxa *Micrococcaceae*/*Micrococcales* (*Actinobacteria*) and *Pseudomonadaceae* (*Proteobacteria*) have reduced resource acquisition traits with a below average (<100 genes) CAZyme count (Fig. 4A). However, there were other drought-selected populations belonging to the taxa *Microbacteriaceae* (*Actinobacteria*), *Sphingomonadaceae* or *Sphingomonadales* (*Proteobacteria*), and *Rhodobacteraceae* (*Proteobacteria*) that maintained a higher CAZyme gene count (>100) while also having higher drought enriched genes (Fig. 4A). This demonstrates that the trade-offs observed in grass litter under

drought were driven by taxonomic differences at the level of family; some of the families identified have been extensively studied at this field site [57, 58].

We then analyzed the temporal dynamics in the abundance of these populations (Fig. 4B) and found that the drought-selected populations with a lower CAZyme count were more abundant at the start of the decomposition process (T1). In contrast, the drought-selected populations with a higher CAZyme count were more abundant at the later time points (T2 to T4). Drought-selected populations in shrub litter did not demonstrate a reduction in CAZyme gene count (Fig. 4A). However, populations belonging to the family *Erwiniaceae* (*Proteobacteria*) that were more abundant at the start of the decomposition process (Fig. 4B) had below average CAZyme count (Fig. 4A) reinforcing that trade-offs were driven by family-level taxonomic differences. However, trait distributions were quite varied in populations within the family *Microbacteriaceae*, which suggests that trade-offs may also occur across populations within a family. Overall, the temporal dynamics in populations and trade-offs between drought tolerance and decomposition capabilities were linked to successional patterns over the litter decomposition process.

Linking population-level traits to decomposition rates

The results from our 18-month decomposition experiment suggest that drought acts as an environmental filter that selects for bacterial populations with a genetic basis for stress tolerance traits that could confer a competitive advantage. We show that in some drought-selected populations, enhanced stress tolerance strategies negatively impacted decomposition capabilities as inferred from CAZyme gene counts. We also observed that the drought-related trade-offs appear across populations, meaning that ecological selection for drought-tolerant taxa can drive trade-offs in traits. Trade-offs may also occur within populations, but further studies with higher resolution MAG assembly and binning would be needed to address the evolutionary processes that underlie such trade-offs.

Our genome-based analysis highlights gene-encoded patterns that likely appear as drought-selected bacterial populations are

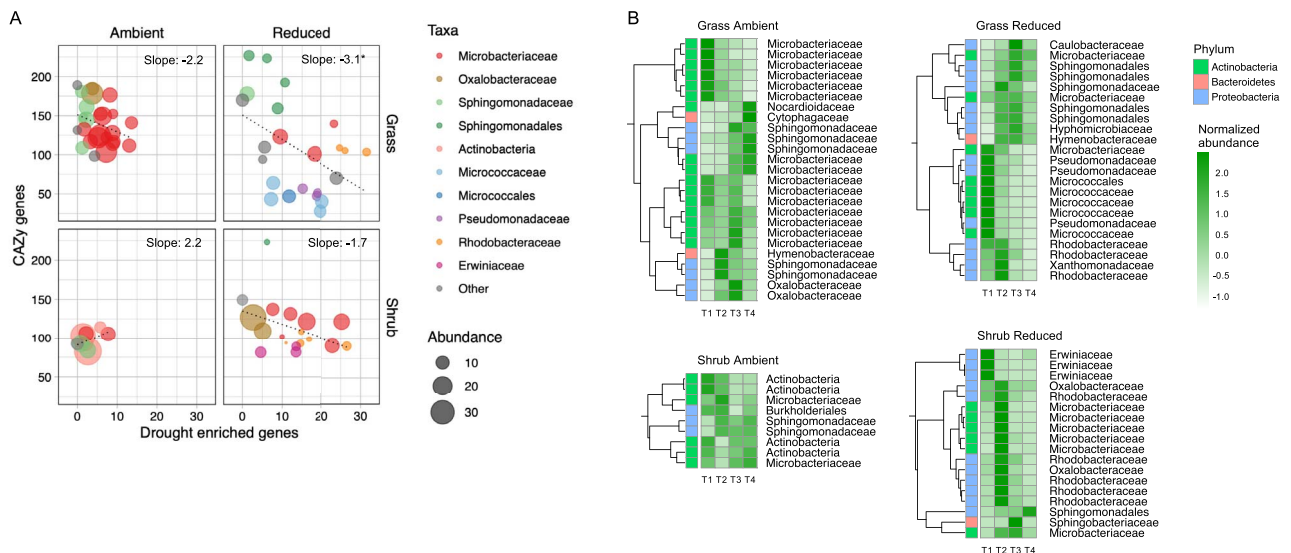


Figure 4. Trade-offs across populations of drought-responsive bacteria. (A) Scatter plot of sum number of genes for all drought-enriched functions in MAGs on the x-axes and total CAZy genes on the y-axes. Displayed here are only those MAGs that were differentially abundant across the precipitation treatments. Each point is a bacterial MAG, and its size represents its mean abundance in metagenomes across all four time points expressed as genome copies per million reads. Linear regression lines and the slope values for each regression are presented. Very low abundance MAGs (<5 genome copies per million reads for bacterial MAGs) were excluded from this analysis. The color represents the taxonomic affiliation of MAGs at the level of family (or order/phylum when that was not available). (B) Heatmaps showing the abundance of the same MAGs at individual time points across all treatments. Similar temporal patterns are clustered together, and the color codes represent their phylum level affiliation.

avored by the decade-long drought imposed in our experiment. Trait trade-offs in response to long-term drought were observed in grass litter and were weak or absent in shrub litter. Tradeoffs between stress tolerance and resource acquisition traits across bacterial populations could reduce decomposition capabilities and ecosystem-level litter decay rates under drought. However, the physiological response of bacteria to drought is only one of the factors that affects decomposition rates. Other factors, such as changes in fungal traits, limitations to resource diffusion and transport, and changes in plant litter chemistry and physico-chemical factors, also affect ecosystem-level decomposition rates [16, 59], which could decouple bacterial population traits from ecosystem process rates. Nevertheless, we show clear links between the metabolism of bacterial populations and collective emergent traits. When integrated into a biogeochemical framework [4], such trait-based scaling can be applied to link the metabolism of microbial populations in a changing environment to the ecosystem functions they perform.

Author contributions

AAM, JBHM, ELB, and SDA designed research; AAM coordinated the project; AAM and CW were involved in litter sampling, experimental setup, sample processing and DNA extractions; AAM, AR, and POS performed bioinformatic analyses; AAM conducted all the statistical analysis; JBHM, ELB, and SDA contributed reagents and analytical tools; AAM drafted the manuscript with inputs from JBHM and SDA; and all authors were involved in critical revision and approval of the final version.

Supplementary material

Supplementary material is available at *The ISME Journal* online.

Conflicts of interest

None declared.

Funding

We acknowledge funding from the US Department of Energy Genomic Science Program, BER, Office of Science projects DE-SC0016410 and DE-SC0020382 awarded to University of California Irvine, and DE-AC02-05CH11231 awarded to Lawrence Berkeley National Laboratory. DNA sequencing was carried out at the DNA Technologies and Expression Analysis Cores at the UC Davis Genome Center, supported by NIH Shared Instrumentation Grant 1S10OD010786-01. Bioinformatics support was available through the Centre for Genome Enabled Biology and Medicine of the University of Aberdeen through an internal Research Enhancement Scheme grant.

Data availability

The sequencing dataset generated and analyzed in the current study are available in the NCBI Sequence Read Archive through BioProject number PRJNA1178105 with accession numbers from SRR31127223 to SRR31127332 (<https://www.ncbi.nlm.nih.gov/sra/PRJNA1178105>).

References

1. Reich PB, Walters MB, Ellsworth DS. From tundra to tundra: global convergence in plant functioning. *Proc Natl Acad Sci* 1997;**94**:13730–4. <https://doi.org/10.1073/pnas.94.25.13730>
2. Wright IJ, Reich PB, Westoby M *et al.* The worldwide leaf economics spectrum. *Nature* 2004;**428**:821–7. <https://doi.org/10.1038/nature02403>
3. Wallenstein MD, Hall EK. A trait-based framework for predicting when and where microbial adaptation to climate change will affect ecosystem functioning. *Biogeochemistry* 2012;**109**:35–47. <https://doi.org/10.1007/s10533-011-9641-8>
4. Hall EK, Bernhardt ES, Bier RL *et al.* Understanding how microbiomes influence the systems they inhabit. *Nat Microbiol* 2018;**3**: 977–82. <https://doi.org/10.1038/s41564-018-0201-z>

5. Malik AA, Puissant J, Buckeridge KM et al. Land use driven change in soil pH affects microbial carbon cycling processes. *Nat Commun* 2018;**9**:3591. <https://doi.org/10.1038/s41467-018-05980-1>
6. Diamond S, Andeer PF, Li Z et al. Mediterranean grassland soil C–N compound turnover is dependent on rainfall and depth, and is mediated by genomically divergent microorganisms. *Nat Microbiol* 2019;**4**:1356–67. <https://doi.org/10.1038/s41564-019-0449-y>
7. Weissman JL, Hou S, Fuhrman JA. Estimating maximal microbial growth rates from cultures, metagenomes, and single cells via codon usage patterns. *Proc Natl Acad Sci* 2021;**118**:e2016810118. <https://doi.org/10.1073/pnas.2016810118>
8. Mackelprang R, Saleska SR, Jacobsen CS et al. Permafrost meta-omics and climate change. *Annu Rev Earth Planet Sci* 2016;**44**:439–62. <https://doi.org/10.1146/annurev-earth-060614-105126>
9. Fierer N. Embracing the unknown: disentangling the complexities of the soil microbiome. *Nat Rev Microbiol* 2017;**15**:579–90. <https://doi.org/10.1038/nrmicro.2017.87>
10. Rocca JD, Hall EK, Lennon JT et al. Relationships between protein-encoding gene abundance and corresponding process are commonly assumed yet rarely observed. *ISME J* 2015;**9**:1693–9. <https://doi.org/10.1038/ismej.2014.252>
11. Fierer N, Barberán A, Laughlin DC. Seeing the forest for the genes: using metagenomics to infer the aggregated traits of microbial communities. *Front Microbiol* 2014;**5**:614. <https://doi.org/10.3389/fmicb.2014.00614>
12. Malik AA, Martiny JB, Brodie EL et al. Defining trait-based microbial strategies with consequences for soil carbon cycling under climate change. *ISME J* 2020;**14**:1–9. <https://doi.org/10.1038/s41396-019-0510-0>
13. Nemergut DR, Schmidt SK, Tadashi F et al. Patterns and processes of microbial community assembly. *Microbiol Mol Biol Rev* 2013;**77**:342–56. <https://doi.org/10.1128/MMBR.00051-12>
14. Martiny JBH, Martiny AC, Brodie E et al. Investigating the eco-evolutionary response of microbiomes to environmental change. *Ecol Lett* 2023;**26**:S81–90. <https://doi.org/10.1111/ele.14209>
15. Manzoni S, Schimel JP, Porporato A. Responses of soil microbial communities to water stress: results from a meta-analysis. *Ecology* 2012;**93**:930–8. <https://doi.org/10.1890/11-0026.1>
16. Schimel JP. Life in dry soils: effects of drought on soil microbial communities and processes. *Annu Rev Ecol Evol Syst* 2018;**49**:409–32.
17. de Vries FT, Liiri ME, Bjørnlund L et al. Legacy effects of drought on plant growth and the soil food web. *Oecologia* 2012;**170**:821–33. <https://doi.org/10.1007/s00442-012-2331-y>
18. Matulich KL, Martiny JBH. Microbial composition alters the response of litter decomposition to environmental change. *Ecology* 2015;**96**:154–63. <https://doi.org/10.1890/14-0357.1>
19. Preece C, Verbruggen E, Liu L et al. Effects of past and current drought on the composition and diversity of soil microbial communities. *Soil Biol Biochem* 2019;**131**:28–39. <https://doi.org/10.1016/j.soilbio.2018.12.022>
20. Lawrence JG, Retchless AC. The interplay of homologous recombination and horizontal gene transfer in bacterial speciation. In: Gogarten M.B., Gogarten J.P., Olendzenski L.C. (eds.), *Horizontal Gene Transfer: Genomes in Flux*. Totowa, NJ: Humana Press, 2009, 29–53.
21. Kimball S, Goulden ML, Suding KN et al. Altered water and nitrogen input shifts succession in a southern California coastal sage community. *Ecol Appl* 2014;**24**:1390–404. <https://doi.org/10.1890/13-1313.1>
22. Allison SD, Lu Y, Weihe C et al. Microbial abundance and composition influence litter decomposition response to environmental change. *Ecology* 2013;**94**:714–25. <https://doi.org/10.1890/12-1243.1>
23. Finks SS, Weihe C, Kimball S et al. Microbial community response to a decade of simulated global changes depends on the plant community. *Elem Sci Anthr* 2021;**9**:00124. <https://doi.org/10.1525/elementa.2021.00124>
24. Meyer F, Paarmann D, D'Souza M et al. The metagenomics RAST server—a public resource for the automatic phylogenetic and functional analysis of metagenomes. *BMC Bioinformatics* 2008;**9**:386. <https://doi.org/10.1186/1471-2105-9-386>
25. Murovec B, Deutsch L, Stres B. Computational framework for high-quality production and large-scale evolutionary analysis of metagenome assembled genomes. *Mol Biol Evol* 2020;**37**:593–8. <https://doi.org/10.1093/molbev/msz237>
26. Li D, Liu C-M, Luo R et al. MEGAHIT: an ultra-fast single-node solution for large and complex metagenomics assembly via succinct de Bruijn graph. *Bioinformatics* 2015;**31**:1674–6. <https://doi.org/10.1093/bioinformatics/btv033>
27. Uritskiy GV, DiRuggiero J, Taylor J. Meta WRAP—a flexible pipeline for genome-resolved metagenomic data analysis. *Microbiome* 2018;**6**:158. <https://doi.org/10.1186/s40168-018-0541-1>
28. Kang DD, Li F, Kirton E et al. MetaBAT 2: an adaptive binning algorithm for robust and efficient genome reconstruction from metagenome assemblies. *PeerJ* 2019;**7**:e7359. <https://doi.org/10.7717/peerj.7359>
29. Alneberg J, Bjarnason BS, de Bruijn I et al. Binning metagenomic contigs by coverage and composition. *Nat Methods* 2014;**11**:1144–6. <https://doi.org/10.1038/nmeth.3103>
30. Wu Y-W, Simmons BA, Singer SW. MaxBin 2.0: an automated binning algorithm to recover genomes from multiple metagenomic datasets. *Bioinformatics* 2016;**32**:605–7. <https://doi.org/10.1093/bioinformatics/btv638>
31. Parks DH, Imelfort M, Skennerton CT et al. CheckM: assessing the quality of microbial genomes recovered from isolates, single cells, and metagenomes. *Genome Res* 2015;**25**:1043–55. <https://doi.org/10.1101/gr.186072.114>
32. Huang L, Zhang H, Wu P et al. dbCAN-seq: a database of carbohydrate-active enzyme (CAZyme) sequence and annotation. *Nucleic Acids Res* 2018;**46**:D516–21. <https://doi.org/10.1093/nar/gkx894>
33. Hyatt D, Chen G-L, LoCascio PF et al. Prodigal: prokaryotic gene recognition and translation initiation site identification. *BMC Bioinformatics* 2010;**11**:119. <https://doi.org/10.1186/1471-2105-11-119>
34. Aramaki T, Blanc-Mathieu R, Endo H et al. KofamKOALA: KEGG Ortholog assignment based on profile HMM and adaptive score threshold. *Bioinformatics* 2020;**36**:2251–2. <https://doi.org/10.1093/bioinformatics/btz859>
35. Love MI, Huber W, Anders S. Moderated estimation of fold change and dispersion for RNA-seq data with DESeq2. *Genome Biol* 2014;**15**:550. <https://doi.org/10.1186/s13059-014-0550-8>
36. Kolde R. Package 'pheatmap', 2019.
37. Wickham H. *ggplot2: Elegant Graphics for Data Analysis*. New York: Springer-Verlag, 2016. <https://doi.org/10.1007/978-3-319-24277-4>
38. R Development Core Team. *R: A Language and Environment for Statistical Computing*, 2017.
39. Jacobson KM, Jacobson PJ. Rainfall regulates decomposition of buried cellulose in the Namib Desert. *J Arid Environ* 1998;**38**:571–83. <https://doi.org/10.1006/jare.1997.0358>
40. Zhang D, Hui D, Luo Y et al. Rates of litter decomposition in terrestrial ecosystems: global patterns and controlling factors. *J Plant Ecol* 2008;**1**:85–93. <https://doi.org/10.1093/jpe/rtn002>

41. Santonja M, Fernandez C, Gauquelin T et al. Climate change effects on litter decomposition: intensive drought leads to a strong decrease of litter mixture interactions. *Plant Soil* 2015;**393**: 69–82. <https://doi.org/10.1007/s11104-015-2471-z>
42. Quer E, Pereira S, Michel T et al. Amplified drought alters leaf litter metabolome, slows down litter decomposition, and modifies home field (dis)advantage in three Mediterranean forests. *Plan Theory* 2022;**11**:2582. <https://doi.org/10.3390/plants11192582>
43. Esch EH, King JY, Cleland EE. Foliar litter chemistry mediates susceptibility to UV degradation in two dominant species from a semi-arid ecosystem. *Plant Soil* 2019;**440**:265–76. <https://doi.org/10.1007/s11104-019-04069-y>
44. Martiny JB, Martiny AC, Weihe C et al. Microbial legacies alter decomposition in response to simulated global change. *ISME J* 2017;**11**:490–9. <https://doi.org/10.1038/ismej.2016.122>
45. Malik AA, Swenson T, Weihe C et al. Drought and plant litter chemistry alter microbial gene expression and metabolite production. *ISME J* 2020;**14**:2236–47. <https://doi.org/10.1038/s41396-020-0683-6>
46. Bouskill NJ, Wood TE, Baran R et al. Belowground response to drought in a tropical Forest soil. I. Changes in microbial functional potential and metabolism. *Front Microbiol* 2016;**7**:525. <https://doi.org/10.3389/fmicb.2016.00525>
47. Pérez Castro S, Cleland EE, Wagner R et al. Soil microbial responses to drought and exotic plants shift carbon metabolism. *ISME J* 2019;**13**:1776–87. <https://doi.org/10.1038/s41396-019-0389-9>
48. Sophie V, Patrick B. NhaA, an Na⁺/H⁺ antiporter involved in environmental survival of vibrio cholerae. *J Bacteriol* 2000;**182**:2937–44. <https://doi.org/10.1128/JB.182.10.2937-2944.2000>
49. Guo W, Li G, Wang N et al. A Na⁺/H⁺ antiporter, K2-NhaD, improves salt and drought tolerance in cotton (*Gossypium hirsutum* L.). *Plant Mol Biol* 2020;**102**:553–67. <https://doi.org/10.1007/s11103-020-00969-1>
50. Tsujii M, Tanudjaja E, Uozumi N. Diverse physiological functions of cation proton antiporters across bacteria and plant cells. *Int J Mol Sci* 2020;**21**:4566. <https://doi.org/10.3390/ijms21124566>
51. Warren CR. Response of osmolytes in soil to drying and rewetting. *Soil Biol Biochem* 2014;**70**:22–32. <https://doi.org/10.1016/j.soilbio.2013.12.008>
52. Bouskill NJ, Wood TE, Baran R et al. Belowground response to drought in a tropical Forest soil. II. Change in microbial function impacts carbon composition. *Front Microbiol* 2016;**7**:323. <https://doi.org/10.3389/fmicb.2016.00323>
53. Bouskill NJ, Lim HC, Borglin S et al. Pre-exposure to drought increases the resistance of tropical forest soil bacterial communities to extended drought. *ISME J* 2013;**7**:384–94. <https://doi.org/10.1038/ismej.2012.113>
54. Jones SE, Pham CA, Zambri MP et al. Streptomyces volatile compounds influence exploration and microbial community dynamics by altering iron availability. *MBio* 2019;**10**: 10.1128/mbio.00171-19. <https://doi.org/10.1128/mBio.00171-19>
55. Xu L, Dong Z, Chiniquy D et al. Genome-resolved metagenomics reveals role of iron metabolism in drought-induced rhizosphere microbiome dynamics. *Nat Commun* 2021;**12**:3209. <https://doi.org/10.1038/s41467-021-23553-7>
56. Drula E, Garron M-L, Dogan S et al. The carbohydrate-active enzyme database: functions and literature. *Nucleic Acids Res* 2022;**50**:D571–7. <https://doi.org/10.1093/nar/gkab1045>
57. Chase AB, Weihe C, Martiny JBH. Adaptive differentiation and rapid evolution of a soil bacterium along a climate gradient. *Proc Natl Acad Sci* 2021;**118**:e2101254118. <https://doi.org/10.1073/pnas.2101254118>
58. Bahareh S, Scales NC, Gaut BS et al. Sphingomonas clade and functional distribution with simulated climate change. *Microbiol Spectr* 2024;**12**:e00236–24. <https://doi.org/10.1128/spectrum.00236-24>
59. Malik AA, Bouskill NJ. Drought impacts on microbial trait distribution and feedback to soil carbon cycling. *Funct Ecol* 2022;**36**: 1442–56. <https://doi.org/10.1111/1365-2435.14010>